(2 H, t, CH_2), 1.96 (4 H, br, CH_2), 3.03 (6 H, s, SCH_3), 4.63 (4 H, s, OCH_2), 5.63 (2 H, br, CH=CH)] was prepared by a modified (longer reaction time, products poured into ice/HCl) literature procedure[52] in 95% yield after recrystallization from MeOH/water (mp 77.5 °C). The reported[17] synthesis of the ditosylate gave only a 35% yield of pure product. 4,4-Bis(bromomethyl)-1-cyclohexene (**18**) [^{1}H NMR][17] was prepared in 90% yield according to a literature method.[53] Anal. Calcd for $C_8H_{12}Br_2$: C, 35.82, H, 4.47; Br, 59.70. Found; C, 35.61; H, 4.69; Br, 59.38. Spiro[2.5]oct-5-ene (**17**) and spiro[2.5]octa-4,6-diene (**4**) were prepared by de Meijere's route[17] and in similar yields. The diene **4** was purified by preparative VPC (with considerable loss) at 100 °C on a 10 ft × $^3/_8$ in. aluminum column packed with 30% carbowax 20 M on chromosorb "W" (40–60 mesh), high performance, acid washed, and dimethylchlorosilane treated.

1,1-Dideuterio-2-phenylethyl bromide was prepared from phenylacetic acid by a literature procedure.[54] All other materials were commercial products.

EPR Spectroscopy. All work was carried out on a Varian E-104 EPR spectrometer with degassed samples. In the laser experiments the light from a Molectron UV-24 nitrogen laser was concentrated but not focussed on the cavity with a quartz lens. Since the beam issuing from the laser has a rectangular cross section with the long axis horizontal, it was first rotated through 90° with two mirrors, so as to put the long axis vertical, thus lighting the sample uniformily. The buildup and decay of **6** after a laser pulse was monitored by terminating the unfiltered but modulated (standard 100-KHz EPR modulation) EPR output into 5000 Ω and into a Nicolet 1170 signal averager. Typically, the signals from 500 laser shots were averaged, giving virtually noise-free traces. The lifetimes could be reproduced to better than ±2%.

Laser Flash Photolysis. To measure the rates of H atoms abstraction, we used a Molectron UV-400 nitrogen laser providing pulses (8 ns, ~3 mJ) at 337.1 nm. The experimental system has been described previously.[55]

The experiments leading to the data in Figures 2 and 3 were carried out by using a frequency doubled ruby laser for excitation. The instrument has been described.[20,21] The monitoring system consists of a pulsed xenon lamp, a monochromator, and an RCA-4840 photomultiplier tube. All samples were deoxygenated by bubbling with oxygen-free argon.

Laser Fluorescence. The experimental system, which has been previously described,[27] makes use of a Molectron DL-300 dye laser pumped by a UV-1000 nitrogen laser for excitation.

Acknowledgments. We are extremely grateful to Professor A. de Meijere for the samples of his spiro[2.5]octa-4,6-diene which got the present work underway. We should also like to thank Dr. R. D. Small, Jr., for his involvement in some of the preliminary laser flash experiments, Dr. J. K. Thomas for the use of his ruby laser system, and Dr. R. Walsh for communicating to us the results of his calculations and for acting as liaison officer.

(52) Buchta, E.; Kröniger, A. *Chimia* **1968**, *22*, 430.
(53) Buchta, E.; Kröniger, A. *Chimia* **1969**, *23*, 225.
(54) Schmid, P.; Bourns, A. N. *Can. J. Chem.* **1975**, *53*, 3513.
(55) Encinas, M. V.; Scaiano, J. C. *J. Am. Chem. Soc.* **1979**, *101*, 2146.

Low-Lying Electronically Excited States of Cycl[3.3.3]azine, a Bridged 12π-Perimeter[1]

Werner Leupin and Jakob Wirz*

Contribution from the Physikalisch-chemisches Institut der Universität Basel, Klingelbergstrasse 80, CH-4056 Basel, Switzerland. *Received March 17, 1980*

Abstract: The previously unnoticed, symmetry-forbidden transition to the lowest excited singlet state S_1 of cycl[3.3.3]azine (**1**) occurs in the near infrared (0.78 μm^{-1}) and the position of this absorption band is very sensitive to inductive perturbations. In a series of aza-substituted derivatives of **1** this band is progressively shifted throughout the visible into the ultraviolet region. The energy difference between the lowest excited singlet and triplet states, S_1 (**1**) and T_1 (**1**), is small and probably negative in violation of Hund's rule. Excitation of **1** to upper excited singlet states gives rise to a moderately intense fluorescence from the degenerate second excited state S_2 ($\phi_f = 3 \times 10^{-3}$). The low-lying electronic states of **1** are described in terms of a simple MO model. Since the frontier orbitals of **1** are localized on two different, alternantly connected sets of atoms, the electronic excitation of **1** is accompanied by a profound redistribution of charge. The concomitant changes in electronic repulsion need to be considered explicitly, at least in a qualitative manner, in order to account for the unusual energetic spacing of the lower electronic states.

Introduction

The synthesis of cycl[3.3.3]azine[2] (**1**) was achieved over 10 years ago by Farquhar and Leaver[3] after a series of unsuccessful attempts by various groups.[2b] In contrast to previous theoretical predictions,[2a,4] **1** was found to be a highly reactive compound, exhibiting a strong paratropic shift in the ^{1}H NMR signals[3,5] and a high propensity toward both oxidation[3,6,7] and reduction.[6] Such properties are characteristic for compounds with a small energy gap between the frontier orbitals (i.e., biradicaloids[8]). Indeed, Dewar and Trinajstić[9] have advanced a simple and convincing

* Dedicated to the memory of Professor Dr. E. Hueckel.
(1) Presented in part at the Swiss Chemical Society Meeting, Bern, Oct 19, 1979, and at the Pacific Conference on Chemistry and Spectroscopy, Pasadena, Calif., Oct 12, 1979 (W. Leupin and J. Wirz, Proceedings of the Pacific Conference on Chemistry and Spectroscopy, Pasadena, Calif., 1979, Abstract No. 235).
(2) (a) IUPAC nomenclature: pyrido[2,1,6-*de*]quinolizine. The cyclazine nomenclature was introduced by R. J. Windgassen, Jr., W. H. Saunders, and V. Boekelheide, *J. Am. Chem. Soc.*, **81**, 1459–1465 (1959). (b) For recent reviews on cyclazine chemistry see A. Taurin, *Chem. Heterocycl. Compd.*, **30**, 245–270 (1977); W. Flitsch and U. Krämer, *Adv. Heterocycl. Chem.*, **22**, 321–365 (1978).
(3) D. Farquhar and D. Leaver, *Chem. Commun.*, 24–25 (1969); D. Farquhar, T. T. Gough, and D. Leaver, *J. Chem. Soc., Perkin Trans. 1*, 341–355 (1976).
(4) R. D. Brown and B. A. W. Coller, *Mol. Phys.*, **2**, 158–168 (1959).
(5) R. C. Haddon, *Tetrahedron*, **28**, 3613–3633, 3635–3655 (1972).
(6) F. Gerson, J. Jachimowicz, and D. Leaver, *J. Am. Chem. Soc.*, **95**, 6702–6708 (1973).
(7) M. H. Palmer, D. Leaver, J. D. Nesbet, R. W. Millar, and R. Egdell, *J. Mol. Struct.*, **42**, 85–101 (1977).
(8) The designation *biradicaloid* asserts that a given molecular structure has, in the MO description, two approximately nonbonding orbitals occupied by a total of two electrons, regardless of the prevailing electronic configuration(s) in the ground state. J. Kolc and J. Michl, *J. Am. Chem. Soc.*, **95**, 7391–7401 (1973).
(9) M. J. S. Dewar and N. Trinajstić, *J. Chem. Soc. A*, 1754–1755 (1969).

0002-7863/80/1502-6068$01.00/0

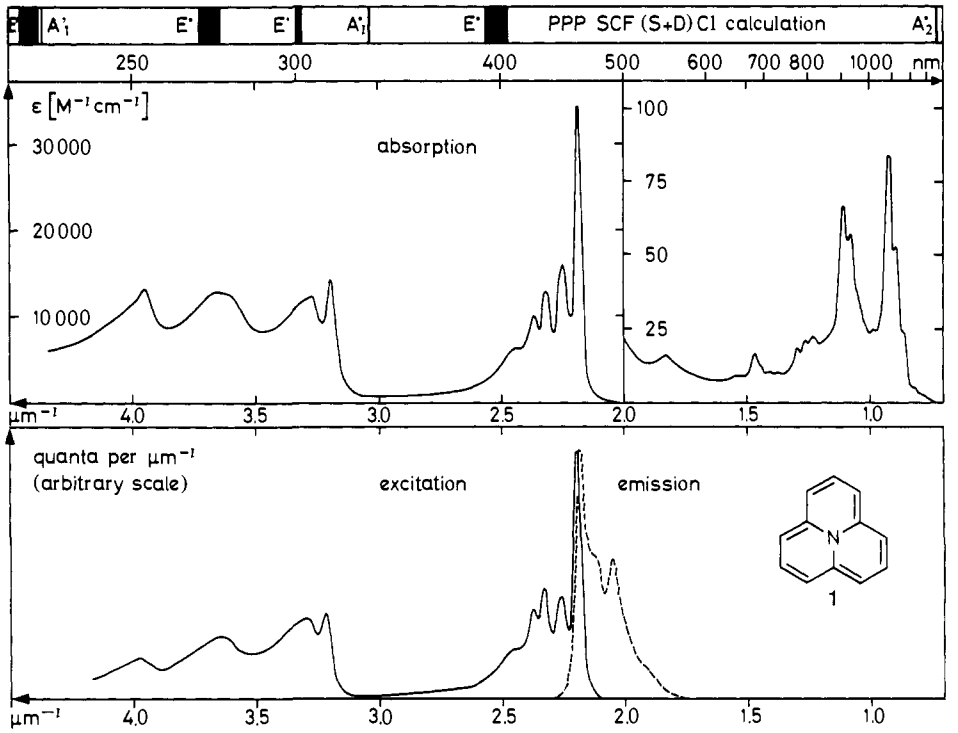

Figure 1. Absorption spectrum (upper half) and corrected emission (dotted) and excitation spectra (lower half) of cycl[3.3.3]azine (**1**) in hexane solution at room temperature. Calculated transitions are shown on top (line thickness indicates transition intensity).

argument to show that **1** is aptly characterized as a nitrogen-bridged, "antiaromatic" [12]annulene (**2**) and that its electronic structure has little in common with the formally isoelectronic, "aromatic" phenalenyl anion ($\mathbf{3}^-$).

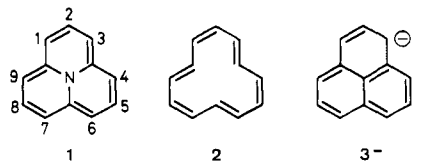

1 2 3⁻

The ubiquitous but fleeting occurrence of biradicaloids as primary photochemical products[10] has stimulated interest in the properties of their low-lying excited states. A number of groups have recently investigated the photophysical properties of various metastable model systems;[11] yet, most experimental studies of [4*n*]annulenes (n = 1, 2, 3, ...)[12] and their derivatives[13] have been focused on ground-state properties. The prediction of biradicaloid character in planar compounds having $4n$ π electrons in cyclic conjugation dates back to 1931 and is now generally referred to as the Hückel ($4n + 2$) rule.[14] We have pointed out[15] that the absorption spectra of planar unsaturated hydrocarbons with a $4n$-membered ring exhibit some systematic features which are quite different from the well-known pattern in the spectra of benzenoid hydrocarbons. Borden and Davidson[16] have drawn attention to some fundamental differences in the electronic structure of conjugated biradicals, depending on whether the NBMOs can or cannot be localized on different sets of atoms. Although a spatial separation of the [4*n*]annulene NBMOs is possible, the splitting induced by perturbations such as bond-length alternation (cyclobutadiene derivatives[12] or trisdehydro[12]annulene **4**[15,17]) or bridging (pyracylene **5**[13]) usually leads to canonical frontier orbitals

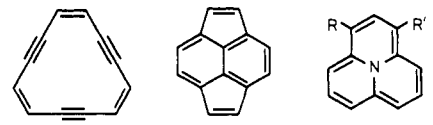

4 5 6

with strong regional overlap. In contrast, the perturbation by the central nitrogen atom in **1** tends to establish the spatial separation of the two frontier orbitals to mutually exclusive regions of the molecule as has been shown by Gerson et al.[6] in an ESR study of the radical anion $\mathbf{1}^-\cdot$ and the radical cation $\mathbf{1}^{+}\cdot$. The present study has disclosed some remarkable features in the photophysical properties of **1** which clearly bear the mark of the frontier-orbital separation in space and support the generalized predictions by Borden and Davidson.

Experimental Section

Di-*tert*-butyl cycl[3.3.3]azine-1,3-dicarboxylate (**6**, R = R′ = CO_2Bu^t) was synthesized and decarboxylated by the published[3] procedures. The precursor compound, di-*tert*-butyl 4*H*-quinolizin-4-ylidenemalonate, was furnished upon special request by Bachem Feinchemikalien AG, CH-4416 Bubendorf, Switzerland. Small samples of the dicarboxylate and the dinitrile (**6**, R = R′ = CN) were available[18] from previous work[6] in these laboratories. The monocarboxylate (**6**, R = H; R′ = CO_2Bu^t) was purified by column chromatography with degassed benzene/petroleum ether on deactivated alumina (0.1 cm³ 10% aqueous acetic acid/g alu-

(10) W. G. Dauben, L. Salem, and N. J. Turro, *Acc. Chem. Res.*, **8**, 41–54 (1975); J. Michl, *Photochem. Photobiol.*, **25**, 141–154 (1977).

(11) Recent leading references: S. L. Buchwalter and G. L. Closs, *J. Am. Chem. Soc.*, **101**, 4688–4694 (1979); M. S. Platz, *ibid.*, **101**, 3398–3399 (1979); M. Gisin, E. Rommel, J. Wirz, M. N. Burnett, and R. M. Pagni, *ibid.*, **101**, 2216–2218 (1979); R. P. Steiner, R. D. Miller, H. J. Dewey, and J. Michl, *ibid.*, **101**, 1820–1826 (1979); N. J. Turro, M. J. Mirbach, N. Harrit, J. A. Berson, and M. S. Platz, *ibid.*, **100**, 7653–7658 (1978); G. Kaupp, E. Teufel, and H. Hopf, *Angew. Chem.*, **91**, 232–234 (1979); *Angew. Chem., Int. Ed. Engl.*, **18**, 215–217 (1979).

(12) G. Maier, *Angew. Chem.*, **86**, 491–505 (1974); *Angew. Chem., Int. Ed. Engl.*, **13**, 425–438 (1974); T. Bally and S. Masamune, *Tetrahedron*, **36**, 343–370 (1980); F. Sondheimer, *Acc. Chem. Res.*, **5**, 81–91 (1972).

(13) B. M. Trost in "Topics in Nonbenzenoid Aromatic Chemistry", Vol. I, Hirokawa Publishing Co., Tokyo, 1973, pp 243–268; B. M. Trost, G. M. Bright, C. Frihart, and D. Britelli, *J. Am. Chem. Soc.*, **93**, 737–745 (1971).

(14) E. Hückel, *Z. Phys.*, **70**, 204–286 (1931); *Z. Elektrochem.*, **43**, 752–788 (1937).

(15) J. Wirz, "Excited States in Organic Chemistry and Biochemistry", *Jerusalem Symp. Quantum Chem. Biochem.*, **10**, 283–294 (1977).

(16) W. T. Borden and E. R. Davidson, *J. Am. Chem. Soc.*, **99**, 4587–4594 (1977); see also H. E. Zimmerman, D. Armesto, M. G. Amezua, T. P. Gannett, and R. P. Johnson, *ibid.*, **101**, 6367–6383 (1979); D. Döhnert and J. Koutecký, *ibid.*, **102**, 1789–1796 (1980).

(17) J. Wirz, *Helv. Chim. Acta*, **59**, 1647–1655 (1976).

(18) We are grateful to Professors F. Gerson and D. Leaver for their permission to use these samples.

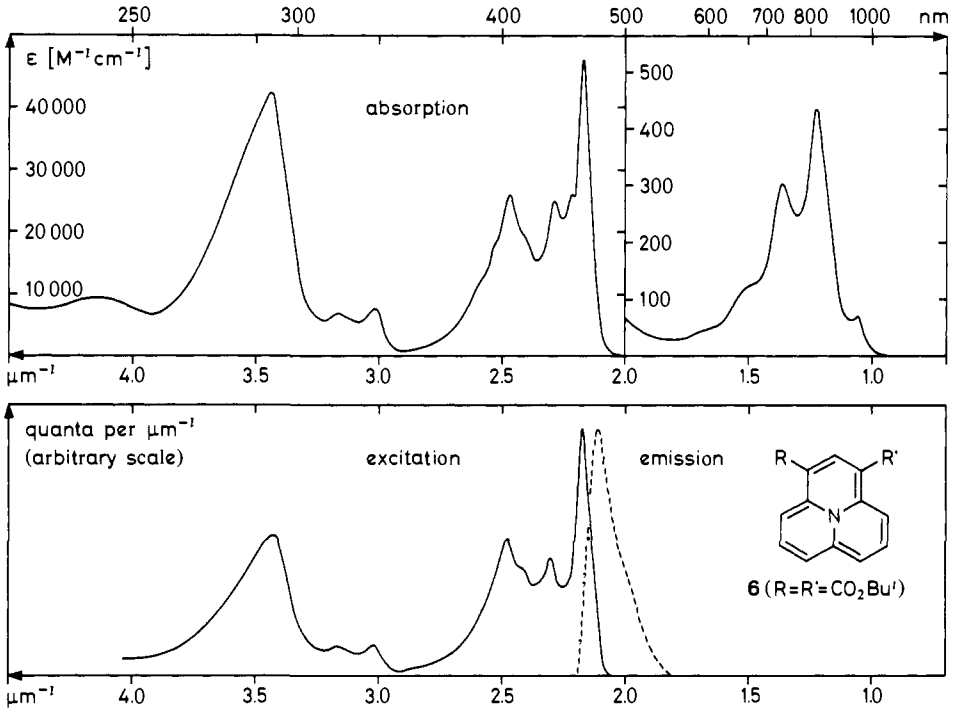

Figure 2. Absorption spectrum (upper half) and corrected emission (dotted) and excitation spectra (lower half) of di-*tert*-butyl cycl[3.3.3]azine-1,3-dicarboxylate (**6**) in hexane solution at room temperature.

mina) and sublimation at 130 °C in vacuo. Parent **1** was purified by repeated vacuum sublimation at 80 °C and recrystallization from degassed petroleum ether at −100 °C. ^{13}C NMR (22.63 MHz, C_6D_6, internal Me_4Si): δ 164.3 (relaxation time > 1.5 s, bridgehead carbons), 141.1 (d, J = 158.7 Hz, C2), 107.3 ppm (dd, J = 165.5 Hz, long-range splittings ca. 5 Hz, C1).

Absorption spectra were measured on a Beckman Acta M IV UV/vis/near-IR spectrometer, and fluorescence and fluorescence excitation spectra on a Schoeffel Instrument Corp. fluorescence spectrometer RRS 1000 equipped with two double monochromators.[19] Fluorescence quantum yields were estimated by comparison of the integrated intensities of the corrected emission spectra with that of a fluorescein standard (0.1 N aqueous sodium hydroxide, 436-nm excitation, $\phi_f \approx 0.90$[20]). Flash photolysis experiments were performed with either a pulsed (20 ns) Nd glass laser (1060 nm, 1 J; frequency tripled 353 nm or quadrupled 265 nm, ca. 50 mJ) or a conventional discharge flashlamp (20 μs, 1000 J) as an excitation source and a kinetic detection system. All experimental data were determined at room temperature with freshly prepared, degassed hexane solutions (fluorescence grade, Merck, Darmstadt) unless otherwise stated.

Results

The absorption, fluorescence emission, and fluorescence excitation spectra of **1** and its dicarboxylate derivative (**6**, R = R′ = CO_2Bu^t) are shown in Figures 1 and 2. Similar results have been obtained for the monocarboxylate (**6**, R = H; R′ = CO_2Bu^t) and the dinitrile (**6**, R = R′ = CN). The fluorescence quantum yields ϕ_f (436-nm excitation) are given in Table I, together with the energies $E(S_1)$ and $E(S_2)$ corresponding to the (apparent) origins of the first and second absorption band, the energy differences $\Delta E(S_2 - S_1)$ between these values, and the radiative rate constants $k_f(S_2)$ calculated by integration of the second absorption band.[21]

The Energy, Lifetime, and Absorption Spectrum of the Lowest Triplet State T_1(1). Flash photolysis of a 10^{-4} M solution of **1** by a 265-nm laser pulse of 20-ns duration gave rise to a transient absorption in the UV (λ_{max} 380 nm) but not in the visible region with a lifetime of ca. 100 ns. Because of the fast decay rate of this transient, we have not been able to identify it unambiguously as an electronically excited species by performing energy-transfer experiments. Nevertheless, the following arguments support its tentative assignment to the triplet state T_1(**1**): (i) No permanent photochemical decomposition is apparent after prolonged irradiation of **1**. Therefore, the decay of the observed transient intermediate eventually leads back to the starting material **1**. (ii) Excitation of **1** to S_1 with a 1060-nm laser pulse does not give rise to any detectable transient changes in the absorption spectrum. Hence the lifetime of S_1, as well as that of S_2 (see Table I), is much shorter than that of the transient observed after 265-nm excitation. (iii) Semiempirical calculations (see below) predict the first intense T_1–T_x transitions at 385 and 336 nm.

Table I. Photophysical Data

compd	$\phi_f(S_2) \times 10^{+3}$	$k_f(S_2) \times 10^{-7}$, s^{-1}	$E(S_1)$, μm^{-1}	$E(S_2)$, μm^{-1}	$\Delta E(S_1 - S_2)$, μm^{-1}
1	3.0 ± 0.4	4[a]	0.784	2.188	1.404
6 (R = H; R′ = CO_2Bu^t)	0.5 ± 0.1	13	0.935	2.086	1.151
6 (R = R′ = CO_2Bu^t)	0.4 ± 0.1	21	1.068	2.172	1.104
6 (R = R′ = CN)[b]	1.1 ± 0.2	17	1.005	2.174	1.169

[a] This value has been halved owing to the degeneracy of S_2.[21] [b] Determined with degassed benzene solutions.

If the assignment of the 380-nm transient to T_1 (**1**) is correct, observation (ii) above indicates that efficient intersystem crossing takes place only from an upper excited singlet state, presumably S_2. Note that the correctness of the above assignment has no bearing on the following determination of the energy of T_1 (**1**).

For obvious reasons, attempts to determine the triplet energy of **1** and its derivatives by phosphorescence emission or heavy atom induced singlet–triplet absorption spectroscopy have not been successful. We have thus resorted to an indirect technique[22] involving the measurement of energy-transfer rates k_{et} from a graded series of triplet sensitizers (benzenoid hydrocarbons with

(19) We wish to thank Professor Dr. K. Kirschner and Dr. S. Tschopp, Biozentrum, Basel, for their help.
(20) J. N. Demas and G. A. Crosby, *J. Phys. Chem.*, **75**, 991–1024 (1971).
(21) S. J. Strickler and R. A. Berg, *J. Chem. Phys.*, **37**, 814–822 (1962).

(22) This technique has, e.g., been used by W. G. Herkstroeter, *J. Am. Chem. Soc.*, 97, 3090–3096, 4161–4167 (1975), and ourselves.[15,27] The triplet energies quoted by Herkstroeter for the low-energy sensitizers pyranthrene, violanthrene, and isoviolanthrene are based on semiempirical calculations. These values appear to be consistently too low by ca. 3 kcal/mol ≃ 0.1 μm^{-1}, as indicated by a correlation between known triplet energies and ^1L_a transition energies for benzenoid hydrocarbons and by the results of open-shell PPP calculations.[29]

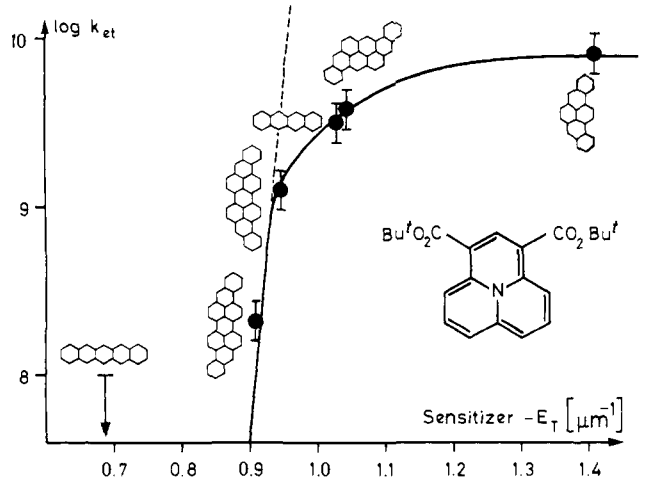

Figure 3. Logarithms of the observed rate constants k_{et} for triplet energy transfer from various benzenoid hydrocarbon sensitizers to **6** (R = R′ = CO_2Bu^t) in benzene solution at room temperature.

differing excitation energies) to the quenchers **1** or **6** (R = R′ = CO_2Bu^t). The rate constants k_{et} were obtained by monitoring the sensitizer decay rates after flash photolysis as a function of added quencher concentration in benzene solution. These rates are known to be close to the diffusion-controlled limit (ca. 1×10^{10} M^{-1} s^{-1}) as long as the energy-transfer process is exothermic, i.e., as long as the vertical deexcitation energy of the sensitizer exceeds the vertical excitation energy of the quencher. They should then fall off rapidly (one decade per 5.7 kJ/mol $\simeq$ 0.05 μm^{-1}) provided that no other quenching process, such as nonvertical quenching[23] or exciplex or electron-transfer quenching,[24] is available. In Figure 3 the quenching rate constants k_{et}, which were determined using the 1,3-dicarboxylate ester (**6**, R = R′ = CO_2Bu^t) as a triplet energy acceptor, are plotted against the triplet energy E_T of the benzenoid sensitizers. The observed quenching rate constants indeed exhibit the expected dependence on E_T of the energy donors. This supports our original assumption that the observed quenching process corresponds to triplet energy transfer. The triplet energy of **6** (R = R′ = CO_2Bu^t) may thus be located[23] near that of isoviolanthrene (E_T = 112 kJ/mol $\simeq$ 0.94 μm^{-1})[22] where k_{et} has dropped to a value of 2×10^8 M^{-1} s^{-1} (Figure 3). Quenching rates with parent **1** were $k_{et} = (3.3 \pm 1.0) \times 10^9$ M^{-1} s^{-1} for violanthrene (E_T = 117 kJ/mol $\simeq$ 0.98 μm^{-1})[22] and $(1.0 \pm 0.5) \times 10^8$ M^{-1} s^{-1} for pentacene (E_T = 83 kJ/mol $\simeq$ 0.69 μm^{-1});[25] i.e., the triplet energy of **1** is estimated as 90 kJ/mol $\simeq$ 0.75 μm^{-1}. Strictly, the above values for E_T of **1** and **6** (R = R′ = CO_2Bu^t) should be considered as lower limits, allowing for the possibility that the observed quenching rates are dominated by processes other than energy transfer. Systematic errors in these values may also arise from errors in the sensitizer triplet energies, but are not likely to exceed ± 0.1 μm^{-1}.

Semiempirical Calculations. Standard PPP SCF (S) CI[26] calculations including all singly excited configurations were performed for **1** in order to predict the transition energies and oscillator strengths of the ground-state absorption spectrum. An idealized D_{3h} molecular geometry (bond lengths 140 pm, bond angles 120°) was assumed and standard[27] parameters were adopted: $I_N - I_C = 15.9$, $\gamma_C = 10.84$, $\gamma_N = 18.0$, $\gamma_{\mu\nu} = 1439.5/(132.8 + R_{\mu\nu})$, $\beta_{CN} = \beta_{CC} = -2.318$ eV. The inclusion of 45 doubly excited configurations, PPP SCF (S + D) CI, without changing the parameter set, had very little influence on the

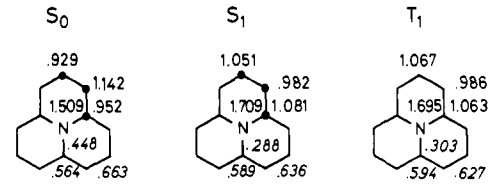

Figure 4. Charge densities and bond orders v calculated by the standard PPP SCF (S) CI procedure for **1** (D_{3h} symmetry assumed).

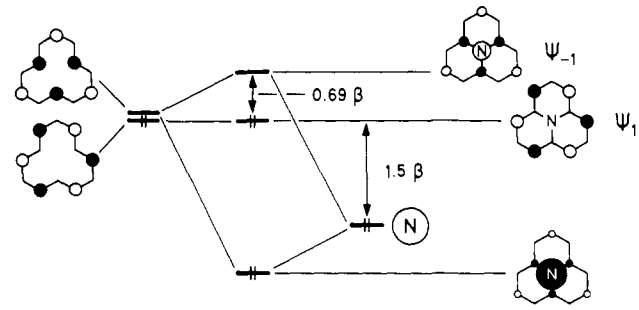

Figure 5. Hückel LCMO scheme to construct the frontier orbitals of **1** from [12]annulene and a nitrogen p lone pair orbital.

calculated absorption spectrum. Furthermore, consideration of the σ-valence electrons in a CNDO SCF (π − S + D) CI calculation using the program by Baumann[28] (same geometry, C–H bond lengths 108 pm, 26 singly and 45 doubly excited configurations, standard parameters provided in the data bank of the program) again gave very similar results.

The triplet–triplet absorption spectrum of **1** was calculated by an open-shell version[29] of the PPP program which performs the SCF calculation for the lowest triplet state. All 22 triplet and 24 singlet configurations arising from single excitation to or from the singly occupied frontier orbitals were included in the CI matrix. The parameters were the same as those used in the closed-shell PPP calculation above. The results of the semiempirical calculations for **1** are summarized in Table II, at the top of Figure 1, and in Figure 4.

Discussion

MO Model. The frontier orbitals of cycl[3.3.3]azine (**1**) are readily obtained by linear combination (LC) of the nonbonding molecular orbitals (NBMOs) of [12]annulene (**2**) with the nitrogen p atomic orbital (AO), as shown in the interaction scheme, Figure 5. Note that the proper choice of NBMOs, which is adapted to the symmetry reduction imposed by the perturbation, corresponds to the spatially separated (localized) pair shown on the left of Figure 5. The frontier orbitals are little changed by performing a full Hückel or SCF calculation for **1**, since, apart from the NBMO considered, only the lowest bonding and highest antibonding π MOs of **2** have the appropriate symmetry to interact with the nitrogen p AO. Using the standard[6] heteroparameter, $\alpha_N = \alpha_C + 1.5\beta$, the energy gap $\Delta\epsilon = \epsilon_{-1} - \epsilon_1$ between the highest occupied orbital (HOMO) ψ_1 and the lowest unoccupied orbital (LUMO) ψ_{-1} is obtained as 0.69β by the LCMO treatment, or 0.63β by a full Hückel calculation. It is reduced to 0.48β by inclusion of an inductive effect arising from the central nitrogen atom on the bridgehead carbon atoms, $\alpha_{C-(N)} = \alpha_C + 0.5\beta$, and increased to 0.78β by assuming alternating bond lengths along the periphery, $\beta_{C=C} = 1.2\beta_0$ and $\beta_{C-C} = 0.8\beta_0$.

Geometry of 1 in the Electronic Ground State. Does the molecule adopt a symmetric (D_{3h}) equilibrium structure (**1a**), or is it stabilized by distorting to, say, a C_{3h} structure (**1b**) with alternating bond lengths along the periphery? Two calculations have yielded double minimum potentials favoring distorted (C_{3h})

(23) V. Balzani, F. Bolletta, and F. Scandola, *J. Am. Chem. Soc.* **102**, 2152–2163 (1980).
(24) R. A. Caldwell, D. Creed, and T.-S. Maw, *J. Am. Chem. Soc.*, **101**, 1293–1295 (1979); G. B. Schuster, *ibid.*, **101**, 5851–5853 (1979).
(25) J. Burgos, M. Pope, C. E. Swenberg, and R. R. Alfano, *Phys. Status Solidi B*, **83**, 249–256 (1977).
(26) R. Pariser and R. G. Parr, *J. Chem. Phys.*, **21**, 466–471 (1953); J. A. Pople, *Trans. Faraday Soc.*, **49**, 1375–1385 (1953).
(27) W. Rettig and J. Wirz, *Helv. Chim. Acta*, **59**, 1054–1074 (1976).
(28) H. Baumann, Quantum Chemistry Program Exchange, Program No. 333, CNDO UV 99 (1978).
(29) M. Gisin and J. Wirz, to be published. A brief description of the program was given by R. Haag, J. Wirz, and P. J. Wagner, *Helv. Chim. Acta*, **60**, 2595–2607 (1977).

Table II. Results of Semiempirical CI Calculations for 1

energy, μm^{-1}	sym D_{3h}	osz strength	coefficients of leading configurations[a]
PPP SCF (S) CI, Singlet States and Lowest Triplet State			
0	$^1A_1'$		1.00 G
0.623	$^3A_2'$	0	0.99(1,−1)
0.703	$^1A_2'$	0	0.99(1,−1)
2.663	$^1E'$	0.526	0.97(1,−2) 0.97(1,−3)
2.736	$^1A_1'$	0	(11,−1−1)[b]
3.920	$^1E'$	0.796	0.94(2,−1) 0.94(3,−1)
4.214	$^1E'$	0.035	0.96(1,−4) 0.96(1,−5)
PPP SCF (S + D) CI, Singlet States Only			
0	$^1A_1'$		0.97 G −0.13[11,−2−2)+(11,−3−3]
0.721	$^1A_2$	0	0.96(1,−1)−0.17[21,−1−2)+ (31,−1−3)]
2.513	$^1E'$	0.163	0.88(1,−2)+0.25(3,−1) 0.88(1,−3)−0.25(2,−1)
3.035	$^1A_1'$	0	0.92(11,−1−1)−0.20[(11,−2−2)+ (11,−3−3)]
3.323	$^1E'$	0.0002	0.62(1,−4)−0.60(11,−2−3) 0.62(1,−5)−0.42[(11,−2−2)− (11,−3−3)]
3.679	$^1E'$	0.316	0.67(11,−1−2)+0.50(2,−1)+ 0.37(1,−3) 0.67(11,−1−3)+0.50(3,−1)− 0.37(1,−2)
CNDO SCF (S + D) CI, Singlet States Only			
0	$^1A_1'$		0.98 G −0.10[(11,−2−2)+(11,−3−3)]
0.749	$^1A_2$	0	0.96(1,−1)−0.16[(21,−1−2)+ (31,−1−3)]
2.534	$^1E'$	0.159	0.91(1,−2)−0.20(3,−1) 0.91(1,−3)+0.20(2,−1)
3.006	$^1A_1'$	0	0.91(11,−1−1)−0.22[(11,−2−2)+ (11,−3−3)]
3.528	$^1E'$	0.0003	0.70(1,−4)−0.52(11,−2−3) 0.70(1,−5)−0.37[(11,−2−2)− (11,−3−3)]
3.753	$^1E'$	0.351	0.73(2,−1)−0.29(1,−3) 0.73(3,−1)+0.29(1,−2)
Open Shell PPP SCF (S) CI, Triplet States and Lowest Singlet States			
−0.544	$^1A_1'$		1.00 G
0[d]	$^3A_2'$		0.99(1,−1)
0.064	$^1A_2'$		0.98(1,−1)
0.790	$^3E'$	0.019[c]	0.98(1,−2) 0.98(1,−3)
1.690	$^3E'$	0.004[c]	0.77(11,−1−2)+0.67(12,−1−1) 0.77(11,−1−3)−0.67(13,−1−1)
2.598	$^3E'$	0.050[c]	0.81(1,−4)−0.4(11,−1−3)−0.4(2,−1) 0.81(1,−5)−0.4(11,−1−2)−0.4(3,−1)
2.873	$^3A_1'$	0[c]	0.98(4,−1)
2.978	$^3E'$	0.428[c]	0.53[(1,−4)+(3,−1)]−0.48 (12,−1−1)+0.44(11,−1−3) 0.53[(1,−5)−(2,−1)]−0.48 (13,−1−1)−0.44(11,−1−2)

[a] π orbitals numbered as usual: bonding orbitals 1 (HOMO), 2,3,. . .; virtual orbitals −1 (LUMO), −2,−3, . . .; the HMO sequence of orbital symmetries is not changed by the SCF calculations. [b] Not included in the CI matrix. [c] Calculated for T_1-T_x transitions. [d] Reference state for T_1-T_x transitions.

over symmetric (D_{3h}) structures by 50 (π SCF MO method with empirical σ-compression energies, optimized geometry)[9] and 30 kJ/mol (GTO ab initio SCF calculation, assumed trial geometries),[7] respectively. On the other hand, the first band in the photoelectron spectrum[7] of **1** appears at very low energy (5.87 eV) and consists of a single, sharp peak with virtually no vibrational progression. This indicates that the electron is ejecten[3]from a truly nonbonding orbital and that the geometries of **1** and its radical cation $\mathbf{1}^{+\cdot}$ are very similar. Since $\mathbf{1}^{+\cdot}$ most likely[6,9] has a symmetrical (D_{3h}) structure, this argues for a single (or very shallow double) minimum potential of **1**. Note that the photoelectron spectra of [4*n*]annulene derivatives with alternating bond lengths exhibit a broad (cyclobutadiene derivatives[30]) or vibrationally structured (trisdehydro[12]annulene **4**[17]) first ionization band at much higher energies. X-ray structure analyses are available only for 4-cyano-2-methyl-1,3,6-triazacycl[3.3.3]azine[31a] and 1,3,4,6-tetraazacycl[3.3.3]azine.[31b] These compounds have "aromatic" bond lengths along the periphery (C–C 138 ± 1, C–N 133 ± 2 pm), but it may be argued that this is due to the stabilizing effect of the peripheral nitrogen atoms. Finally, the NMR spectra of **1** (^{1}H NMR,[3] ^{13}C NMR see Experimental Section) are consistent with either **1a** or a rapid isodynamic equilibrium **1b** ⇌ **1c**.

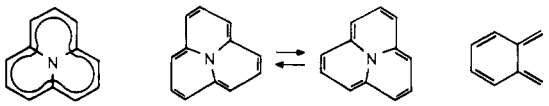

1a **1b** **1c** **7**

In the absence of more direct evidence, we have assumed standard "aromatic" bond lengths for our semiempirical calculations and have thus obtained good agreement with the experimental data.

Electronic Absorption Spectrum of 1. The bright yellow color of solutions containing **1** is due to an intense absorption band at $\lambda \leq 458$ nm (2.19 μm^{-1}, prominent 0–0 band, log ϵ 4.45)[3] which hitherto was tacitly assumed to correspond to the lowest energy transition. It was, however, noted[3] with surprise that the position of this band is rather insensitive to substitution by electronegative groups at the 1 and 3 position (derivatives **6**), in contrast to the large electronic perturbation revealed by the paratropic shift in the ^{1}H NMR spectra. Returning to the simple HMO model presented above, we note first that the calculated energy $\Delta\epsilon$ of ca. 0.6β (±0.2β, depending on the choice of parameters) between the frontier orbitals of **1** appears to be in excellent agreement with the energy of the transition at 2.18 μm^{-1}, since the first absorption bands of *o*-xylylene (**7**)[32] or tetracene, both having a HOMO–LUMO gap $\Delta\epsilon$ of 0.59β, lie in the same spectral region (2.5 and 2.1 μm^{-1}, respectively). However, the excited configuration corresponding to HOMO → LUMO excitation of **1** belongs to the A_2' (D_{3h}) or A′ (C_{3h}) irreducible representation and cannot be associated with the allowed transition at 2.18 μm^{-1}. In fact, the corresponding transition has been observed at $\lambda \leq 1290$ nm (0.78 μm^{-1}, Figure 1). Various semiempirical SCF CI calculations (Table II and top of Figure 1) correctly predict a forbidden S_0–S_1 transition in the near-infrared region. These calculations also predict an optically allowed, degenerate S_2 state near 2.5 μm^{-1} belonging to the E′ irreducible representation. As expected, the corresponding absorption band is split into two separate transitions in substituted derivatives of lower symmetry, e.g., **6** (R = R′ = CO_2Bu^t), Figure 2.

The failure of Hückel theory to reproduce the threefold change in energy between the S_0–S_1 transitions of **7** (2.5 μm^{-1}) and **1** (0.78 μm^{-1}) can be understood by a qualitative consideration of the relevant electron interaction terms. A general discussion of such effects in conjugated biradicals has been given by Borden and Davidson,[16] and a number of particular examples have been analyzed previously.[33] Hückel theory, in spite of its well-known deficiencies, is generally used as a valuable guideline in all kinds of chemical problems. It is thus useful to acquire an intuitive feeling for important effects ignored by the model, rather than to rely on the results of more sophisticated "black box" calculations for individual cases.

(30) E. Heilbronner, T. B. Jones, A. Krebs, G. Maier, K.-D. Malsch, J. Pocklington, and A. Schmelzer, *J. Am. Chem. Soc.*, **102**, 564–568 (1980).
(31) (a) C. C. T. Chiang, *Diss. Abstr. Int. B*, **36**, 2238 (1975); (b) O. Lindqvist, E. Ljungström, E. Andréasson, and O. Ceder, *Acta Crystallogr., Sect. B*, **34**, 1667–1670 (1978).
(32) C. R. Flynn and J. Michl, *J. Am. Chem. Soc.*, **96**, 3280–3288 (1974); E. Migirdicyan and J. Baudet, *ibid.*, 97, 7400–7404 (1975).
(33) (a) P. Baumgartner, E. Weltin, G. Wagnière, and E. Heilbronner, *Helv. Chim. Acta*, **48**, 751–764 (1965); (b) E. Haselbach, Z. Lanyiova, M. Rossi, and A. Schmelzer, *Chimia*, **28**, 19 (1974); (c) J. Michl and R. S. Becker, *J. Chem. Phys.*, **46**, 3889–3894 (1967); J. Michl and E. W. Thulstrup, *Tetrahedron*, **32**, 205–209 (1976); (d) M. A. Souto, D. Otteson, and J. Michl, *J. Am. Chem. Soc.*, **100**, 6892–6898 (1978).

Effects of Electron Repulsion. Consider the low-energy electronic configurations of a biradicaloid system which may be constructed by single and double excitation within the frontier orbitals, i.e., from the HOMO ψ_1 to the LUMO ψ_{-1}. These are the singlet ground configuration $^1\chi_G$, the singly excited singlet and triplet configurations $^1\chi_1^{-1}$ and $^3\chi_1^{-1}$, and the doubly excited singlet configuration $^1\chi_{11}^{-1-1}$. Taking proper account of the changes in electronic repulsion upon excitation, the energies of these configurations are as follows:[34]

$$\begin{aligned} E(^1\chi_G) &\equiv 0 \text{ (by definition)} \\ E(^1\chi_1^{-1}) &= \epsilon_{-1} - \epsilon_1 - J_{1-1} + 2K_{1-1} \\ E(^3\chi_1^{-1}) &= \epsilon_{-1} - \epsilon_1 - J_{1-1} \\ E(^1\chi_{11}^{-1-1}) &= 2\epsilon_{-1} - 2\epsilon_1 - 4J_{1-1} + J_{11} + J_{-1-1} + 2K_{1-1} \end{aligned} \quad (1)$$

The Coulomb repulsion integrals J_{ij} and the exchange integrals K_{ij} are defined as usual:

$$J_{ij} = \int \psi_i^*(1)\psi_j^*(2)(e^2/r_{12})\psi_i(1)\psi_j(2)\, d\upsilon = \sum_\mu \sum_\nu c_{i\mu}^2 c_{j\nu}^2 \gamma_{\mu\nu}$$

$$K_{ij} = \int \psi_i^*(1)\psi_j^*(2)(e^2/r_{12})\psi_j(1)\psi_i(2)\, d\upsilon = \sum_\mu \sum_\nu c_{i\mu}c_{j\nu}c_{j\mu}c_{i\nu}\gamma_{\mu\nu} \quad (2)$$

where the expansion into Coulomb repulsion integrals $\gamma_{\mu\nu}$ between the atomic orbitals ϕ_μ and ϕ_ν makes use of the zero differential overlap approximation,[26] $\phi_\mu\phi_\nu = 0$ for $\mu \neq \nu$.

Although the orbital energy differences in (1) implicitly include numerous repulsion and exchange integrals, these will cancel, if we consider only differences in energy between excited configurations. Hence, the important electron interaction terms are those involving the frontier orbitals ψ_1 and ψ_{-1}. Because of the spatial localization of ψ_1 and ψ_{-1} on two different sets of atoms in **1** (Figure 5), the exchange integral K_{1-1} must vanish within the ZDO approximation, because each term in expansion (2) contains two zero coefficients. For the same reason, the interorbital repulsion integral J_{1-1} does not contain any contributions from monoatomic terms $\gamma_{\mu\mu}$ and is considerably smaller than the intraorbital repulsion integrals J_{11} and J_{-1-1}. We thus arrive at the following relations:

$$\begin{aligned} E(^1\chi_1^{-1}) - E(^3\chi_1^{-1}) &= 0 \\ E(^1\chi_{11}^{-1-1}) - 2E(^1\chi_1^{-1}) &= -2J_{1-1} + J_{11} + J_{-1-1} > 0 \end{aligned} \quad (3)$$

While configuration interaction within the singlet manifold is frequently of importance in biradicaloid systems, this is not the case for **1**. For D_{3h} molecular symmetry, the singly excited configuration $^1\chi_1^{-1}$ belongs to a different representation (A_2') than the totally symmetric (A_1') configurations $^1\chi_G$ and $^1\chi_{11}^{-1-1}$, and the interaction between the latter, $\langle ^1\chi_G(e^2/r_{12})^1\chi_{11}^{-1-1}\rangle = K_{1-1}$, is zero as shown above. The configurations used are therefore good representations of the molecular states $S_0 \simeq {}^1\chi_G$, $S_1 \simeq {}^1\chi_1^{-1}$, $T_1 \simeq {}^3\chi_1^{-1}$, and $S_D \simeq {}^1\chi_{11}^{-1-1}$.

The situation is quite different for an alternant hydrocarbon such as *o*-xylylene (**7**). Here the exchange integral K_{1-1} is quite large (ca. 1 eV)[35] and the repulsion integrals J_{11}, J_{1-1}, and J_{-1-1} are all equal as a consequence of the pairing properties of ψ_1 and ψ_{-1}. The resulting relations corresponding to (3) are

$$\begin{aligned} E(^1\chi_1^{-1}) - E(^3\chi_1^{-1}) &= 2K_{1-1} \gg 0 \\ E(^1\chi_{11}^{-1-1}) - 2E(^1\chi_1^{-1}) &= -2K_{1-1} \ll 0 \end{aligned} \quad (4)$$

In this case, the interaction between the ground and the doubly excited configuration, $\langle ^1\chi_G(e^2/r_{12})^1\chi_{11}^{-1-1}\rangle = K_{1-1}$, leads to a sizable stabilization of the ground state S_0.[35]

The above qualitative rules (3) and (4) are substantiated by explicit SCF calculations with extensive CI (Table II and, e.g., ref 32 and 36) and allow the following conclusions concerning excited-state energies: *spatially separated frontier orbitals* (excitation associated with charge reorganization), $S_D \gg S_1 \approx T_1$; *paired frontier orbitals* (alternant hydrocarbons), $S_D \approx S_1 \gg T_1$. In view of the importance of these states in photochemical reactions, these qualitative rules are worth keeping in mind.

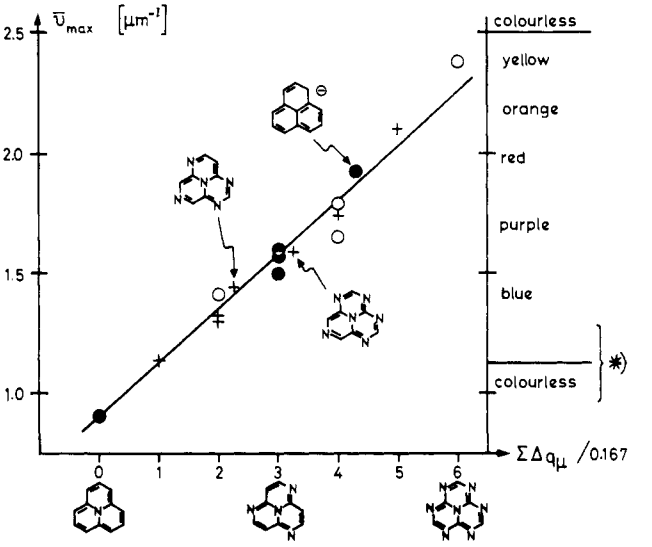

Figure 6. Inductive perturbation of the S_0–S_1 transition of **1**. The transition energies of aza-substituted cycl[3.3.3]azines[38,39] are plotted vs. Hückel charge density changes upon excitation, $\Delta_{q_\mu}(\mathbf{1})$, summed over the substituted centers μ (eq 5). For some polyaza derivatives several isomers are known. In the case of perinaphthenyl anion the Δq value at the central atom was counted threefold, since $\delta\alpha(\dot{N}) = 3\delta\alpha(\dot{N}) = 1.5\beta$. Full circles (●) indicate the energy of the first prominent vibrational peak in known parent compounds. Empty circles (○) refer to extrapolated values (corrected for additional exocyclic substituents, see text) and crosses (+) refer to (extrapolated) values, where only an estimate of $\bar{\nu}_{max}$ was available from colors quoted in the literature. The asterisk indicates compounds with $\bar{\nu}_{max}(S_1) \lesssim 1.4\ \mu m^{-1}$ which are usually green or yellow due to the second absorption band being shifted into the visible region ($\bar{\nu}_{max}(S_2) < 2.2\ \mu m^{-1}$).

Inductive Effects on the S_0–S_1 Transition. The spatial separation of the frontier orbitals and the consequent charge redistribution upon S_0–S_1 excitation of **1** are clearly manifested in the sensitivity of the transition energy to inductive perturbation. On the basis of first-order perturbation theory[37] we expect a hypsochromic shift, $\delta E(S_1) > 0$, upon substitution by inductive acceptors (e.g., CH → N, or H → CO_2R) in positions μ = 1, 3, etc., or by inductive donors (H → CH_3) in positions μ = 2, 5, 8, and vice versa:

$$\delta E(S_1) = \sum_\mu \Delta q_\mu \delta\alpha_\mu = \sum_\mu (c_{1\mu}^2 - c_{-1\mu}^2)\delta\alpha_\mu \quad (5)$$

Taking the frontier orbital coefficients $c_{1\mu}$ and $c_{-1\mu}$ from the LCMO treatment (Figure 5), the change in charge density Δq_μ upon excitation to S_1 equals +0.167 (μ = 1, 3, ...) and −0.127 (μ = 2, 5, 8). Although numerous derivatives of cycl[3.3.3]azine are known,[2b] the position of the first absorption band is properly documented only in the work of Ceder et al.[38a] A few λ_{max} values have been quoted[38b] and in other cases the position of the first band may be roughly estimated from the reported color of the compounds. We have found that, whenever the literature data allow a comparison of the S_0–S_1 transition energy in two related cycl[3.3.3]azine derivatives, the prediction obtained from eq 5 is qualitatively correct.

(34) J. N. Murrell and K. L. McEwen, *J. Chem. Phys.*, **25**, 1143–1149 (1956).
(35) P. Forster, R. Gschwind, E. Haselbach, U. Klemm, and J. Wirz, *Nouveau J. Chim.*, **4**, 365–367 (1980).
(36) P. Tavan and K. Schulten, *J. Chem. Phys.*, **70**, 5407–5413, 5414–5421 (1979).
(37) H. C. Longuet-Higgins and R. G. Sowden, *J. Chem. Soc.*, 1404–1408 (1952).
(38) (a) O. Ceder and J. E. Andersson, *Acta Chem. Scand.*, **26**, 596–610 (1972); O. Ceder and J. F. Witte, *ibid.*, **26**, 635–643 (1972); O. Ceder and K. Rosén, *ibid.*, **27**, 2421–2425 (1973); O. Ceder and K. Vernmark, *Acta Chem. Scand., Ser. B*, **31**, 235–238 (1977); (b) M. Matsuo, H. Awaya, C. Maseda, Y. Tominaga, R. Natsuki, Y. Matsuda, and G. Kobayashi, *Chem. Pharm. Bull.*, **22**, 2765–2766 (1974).

As an illustration, we have collected the available[39] data on aza-substituted cycl[3.3.3]azines in Figure 6, where the position of the first absorption band (first prominent vibrational peak) is plotted against $\sum \Delta q_\mu$. When only derivatives of a given aza-cycl[3.3.3]azine have been reported, the observed transition energy was corrected for the substituent effect on the basis of eq 5; the necessary shift parameters $\delta\alpha_\mu(CO_2R) = 0.6$, $\delta\alpha_\mu(CN) = 0.3$, and $\delta\alpha_\mu(CH_3) = -0.4\ \mu m^{-1}$ were derived from other pairs, where data on both the parent and substituted cyclazine were available.

In view of the pragmatic and somewhat arbitrary treatment of data from various sources, we cannot make any claim about the precision of eq 5 and the shift parameters involved. Nevertheless, the shift of the S_0–S_1 transition from the near infrared in **1** to the near ultraviolet in the cyamelurine derivatives (**8**) is remarkable and the qualitative value of eq 5 is obvious. The slope of the regression line corresponds to a shift parameter $\delta\alpha_\mu(N) = 1.3\ \mu m^{-1}$. Extrapolation from **1** to the (unknown) triaza derivative **9** yields the entertaining prediction $E(S_1) \simeq E(S_0)$.

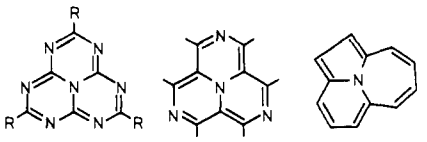

8 9 10

Also worth noting is the dramatic increase in chemical stability which accompanies the progressive shift in the S_0–S_1 transition energy. Whereas the parent compound **1**, let alone the unknown derivative **9**, is a highly reactive, air-sensitive compound, the derivatives of cyamelurine (**8**)[40] are formed by high-temperature pyrolysis reactions and are used as heat-stable additives to produce fireproof coatings.

Energy of the Lowest Triplet State T_1 (1). Based on the observation that the rate constant for the quenching of pentacene triplet ($E_T \simeq 0.69\ \mu m^{-1}$)[25] by **1** is two orders of magnitude below the diffusion-controlled limit, we may definitely locate T_1 (**1**) above $0.6\ \mu m^{-1}$. From the results of a series of energy-transfer experiments with **1** and the diester **6** (R = R′ = CO_2Bu^t) (Figure 3) we estimate a value E_T (**1**) $\simeq 0.7_5 \pm 0.1\ \mu m^{-1}$. It is in fact likely[41] that the energy of T_1 is slightly higher than that of S_1, E_S (**1**) = $0.78\ \mu m^{-1}$, but in any case the energy gap between S_1 and T_1 must be small ($\lesssim 0.1\ \mu m^{-1}$). Thus the availability of a nearly isoenergetic decay path for T_1 (intersystem crossing to S_1) may be responsible for its short lifetime of 100 ns. The reader may be surprised that two states of different multiplicity, which both are well described by the same π,π^* configuration, should have nearly the same energy. For comparison, an energy gap $E(S_1)$–$E(T_1)$ corresponding to ca. $1\ \mu m^{-1}$ is found in benzenoid hydrocarbons of similar size.[42] This is a further manifestation of the frontier orbital localization which confirms the prediction of eq 3. A much larger energy gap may be expected for the isomeric cycl[4.3.2]azine (**10**) which has delocalized frontier orbitals. On the basis of PPP calculations we predict E_S (**10**) $\simeq 1.4$ and E_T (**10**) $\simeq 0.5\ \mu m^{-1}$. The presence of a thermally accessible triplet state may be responsible for the failure of recent efforts[43] to isolate parent **10**.

Fluorescence Emission from the S_2 State and the Energy of the "Doubly Excited" S_D State. The S_2–S_0 fluorescence emission spectra of **1** and **6** (R = R′ = CO_2Bu^t) are shown in Figures 1 and 2. Attempts to detect luminescence attributable to S_2–S_1 fluorescence at $\lambda \geq 710$ nm [$\Delta E(S_2$–$S_1) \simeq 1.4\ \mu m^{-1}$, Table I] using our conventional instrumentation have failed. The S_2–S_0 fluorescence of **1** with a quantum yield of 3×10^{-3} (Table I) represents a violation of Kasha's rule[44] and examples of such behavior are quite rare.[45] Apart from the well-known case of azulene and its derivatives, S_2 fluorescence of [**18**]annulene[46] and of thioketones[45] has been noted as an exception. Strong emission from excited radical ions of benzene derivatives with a degenerate or nearly degenerate ground state has also been observed.[47] We should add that very weak fluorescence emission from upper excited singlet states ($\phi_f \lesssim 10^{-5}$) may be expected to occur quite commonly, and in fact examples are now being routinely detected with sophisticated instrumentation.[48]

Numerous reports of S_2–S_0 fluorescence did not withstand subsequent scrutiny and have been shown to be artifacts, mostly due to impurity emission. We feel that the following evidence is sufficient to establish the observed luminescence as an authentic S_2–S_0 emission of **1**: (i) Emission was observed with all derivatives **6** which have been investigated (Table I). Some of these samples were available from two different sources.[18] In addition, 1,4,7-triazacycl[3.3.3]azine and its 2,5,8-trimethyl derivative,[39] which are obtained by a completely different synthetic route, were also found to exhibit weak S_2–S_0 fluorescence. (ii) Ignoring some loss in vibrational structure, the emission spectra are an approximate mirror image of the S_0–S_2 absorption band and the 0–0 bands of absorption and emission are nearly coincident in all cases (Figures 1 and 2). Note that the degenerate S_0–S_2 transition of **1** is split into two partially overlapping bands in the derivatives **6** and that the emission spectrum mirrors only the lower energy band, as expected. (iii) The corrected fluorescence excitation spectra (Figures 1 and 2) were in satisfactory agreement with the absorption spectra. (iv) Repeated purification by various procedures or prolonged irradiation of the samples did not give any detectable changes in the emission or excitation spectra.

The optically forbidden S_D state of **1**, which is described by the doubly excited leading configuration χ_{11}^{-1-1}, appears to be located at higher energy than that of the allowed S_0–S_2 transition ($2.18\ \mu m^{-1}$). This statement is supported not only by the absence[49] of any detectable transition in the optical window below $2.18\ \mu m^{-1}$, but also by the observation of S_2–S_0 emission and the dependence of its quantum yield on the energy gap $\Delta E(S_1$–$S_2)$ (Table I). The presence of an optically forbidden S_D state below S_2 would be expected to provide a rapid radiationless decay channel for the S_2 state. Thus the energy of the S_D state appears to be at least three times that of the corresponding "singly excited" S_1 state ($0.78\ \mu m^{-1}$), in agreement with the qualitative prediction of eq 3 and the semiempirical calculations (Table II, Figure 1). Conversely, in alternant hydrocarbons the two singlet states associated with single and double HOMO → LUMO excitation,

(39) In addition to the data given in ref 2b and 38 we have included the spectrum of 1,4,7-triazacycl[3.3.3]azine and its 2,5,8-trimethyl derivative: W. Leupin and J. Wirz, unpublished results.

(40) L. Pauling and J. H. Sturdivant, *Proc. Natl. Acad. Sci. U.S.A.*, **23**, 615–620 (1973); H. Schroeder and E. Kober, *J. Org. Chem.*, **27**, 4262–4266 (1962).

(41) Our open-shell PPP calculations for **1** (Table 1) predict $E_S - E_T = +0.06\ \mu m^{-1}$. The small stabilization of T_1 arises from a slight regional overlap of the SCF frontier MOs. However, based on the results of extensive ab initio CI calculations for the related case of square cyclobutadiene (references below), it may be expected that more elaborate calculations for **1** would tend to stabilize S_1 relative to T_1 by "dynamic spin polarization" and lead to a violation of Hund's rule, i.e., $E_S - E_T < 0$, even at D_{3h} geometry. W. T. Borden, *J. Am. Chem. Soc.*, 97, 5968–5970 (1975); H. Kollmar and V. Staemmler, *ibid.*, 99, 3583–3587 (1977); H. Kollmar and V. Staemmler, *Theor. Chim. Acta*, **48**, 223–239 (1978); W. T. Borden, E. R. Davidson, and P. Hart, *J. Am. Chem. Soc.*, **100**, 388–392 (1978); J. A. Jafri and M. D. Newton, *ibid.*, **100**, 5012–5017 (1978).

(42) A case related[33c] to that of **1** is azulene, for which $E_S - E_T = 0.08\ \mu m^{-1}$ has been determined: P. Kroening, *Z. Phys. Chem.* (*Frankfurt am Main*), **86**, 225–229 (1973); ref 22.

(43) W. Flitsch and E. Mukidjam, *Chem. Ber.*, **112**, 3577–3588 (1979).

(44) M. Kasha, *Discuss. Faraday Soc.*, 9, 14–19 (1950).

(45) N. J. Turro, V. Ramamurthy, W. Cherry, and W. Farneth, *Chem. Rev.*, **78**, 125–145 (1978).

(46) U. P. Wild, H. J. Griesser, Vo Dinh Tuan, and J. F. M. Oth, *Chem. Phys. Lett.*, **41**, 450–455 (1976).

(47) M. Allan, J. P. Maier, and O. Marthaler, *Chem. Phys.*, **26**, 131–140 (1977); G. Dujardin, S. Leach, and G. Taieb, *ibid.*, **46**, 407–421 (1980).

(48) B. Nickel and G. Roden, *Ber. Bunsenges. Phys. Chem.*, **81**, 281–285 (1977); B. Nickel, *Helv. Chim. Acta*, **61**, 198–222 (1978); V. Rehak, A. Novak, and M. Titz, *Chem. Phys. Lett.*, **52**, 39–42 (1977); H.-B. Lin and M. Topp, *ibid.*, **64**, 452–456 (1979); **67**, 273–278 (1979); C. G. Morgante and W. S. Struve, *ibid.*, **68**, 267–271 (1979); B. F. Plummer, M. J. Hopkinson, and J. H. Zoeller, *J. Am. Chem. Soc.*, **101**, 6779–6781 (1979).

(49) The weak feature at $1.83\ \mu m^{-1}$ in the absorption spectrum of **1** (Figure 1) is attributed to an impurity. The intensity of this peak differed from batch to batch and was completely absent in a single sample which had been dissolved in benzene.

respectively, are of comparable energy (eq 4 and ref 36). In fact, the "doubly excited" state was found[50] to be the lowest excited singlet state in some systems with a small HOMO–LUMO energy gap $\Delta\epsilon$, and a large number of photoreactions initiated in the S_1 state are assumed to proceed via a "pericyclic minimum" of S_D character.[51]

Acknowledgments. This work is part of Project 2.012-0.78 of the Swiss National Science Foundation. Financial support from Ciba-Geigy SA, Hoffmann-La Roche SA, Sandoz SA, and the "Ciba-Stiftung" is gratefully acknowledged.

(50) B. S. Hudson and B. E. Kohler, *Chem. Phys. Lett.*, **14**, 299–305 (1972); R. P. Steiner, R. D. Miller, H. J. Dewey, and J. Michl, *J. Am. Chem. Soc.*, **101**, 1820–1826 (1979); see also ref 36.

(51) See ref 10 and, e.g., J. Michl, *Pure Appl. Chem.*, **41**, 507–534 (1975).

Equilibria and Absorption Spectra of Schiff Bases[1]

Carol M. Metzler, Allen Cahill, and David E. Metzler*

Contribution from the Department of Biochemistry and Biophysics, Iowa State University, Ames, Iowa 50011. *Received March 21, 1980*

Abstract: Equilibria in the formation of Schiff bases between eight aromatic aldehydes including salicylaldehyde and pyridoxal 5′-phosphate with a variety of different amines, diamines, and amino acids have been investigated. The formation constants, the acid dissociation constants of the Schiff bases, and the absorption spectra of the various ionic species of the Schiff bases have been evaluated. The spectra have been resolved into components with log normal curves to provide a precise description of the band shapes and to permit estimation of tautomerization constants. Constants for ring closure in the Schiff bases of diamines have also been estimated. In addition to the major tautomer, which has an ortho quinonoid structure, smaller amounts of both a phenolic tautomer and a tautomer with a dipolar ionic pyridine ring are present in small amounts. Results of this study are correlated with those of previous investigations on related systems and with spectra of two enzymes.

Familiarity with the properties of Schiff bases (imines) of pyridoxal 5′-phosphate (**6**) with amines and amino acids is basic to an understanding of the function of this coenzyme in biological catalysis. It is also of importance because of the growing interest in using **6** and related materials as reagents for the modification of enzymes and other proteins. Numerous papers dealing with these Schiff bases have appeared. There is also a voluminous literature on the closely related Schiff bases of salicylaldehyde (**1**). However, because of the complexity of the ionic equilibrium needed to describe Schiff base forming systems, relatively few quantitative studies have appeared.

In this paper we provide a systematic description of 20 systems based on aldehydes **1**–**8**. Formation constants, acid dissociation constants, and absorption spectra of the individual ionic forms of the Schiff bases have been evaluated from absorption spectra using previously described computer-assisted methods.[2-6]

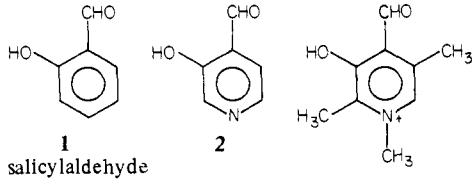

1
salicylaldehyde

2

4

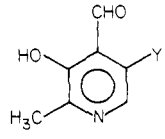

Y

3	CH_3	5-deoxypyridoxal
5	CH_2OH	pyridoxal
6	CH_2OPO^{2-}	pyridoxal 5′-phosphate
7	CH_2OSO^{3-}	pyridoxal 5′-sulfate
8	$CH_2PO_3^{2-}$	

Experimental Section

Chemicals. Commercial amino acids, amines, and inorganic chemicals were used. Salicylaldehyde (**1**) (Aldrich Chemical Co., 98% pure) was distilled under vacuum at 25 °C to give a colorless product. 3-Hydroxy-4-pyridinaldehyde (**2**) was a gift from Dr. Marion O'Leary. The following were synthesized as described previously: 5-deoxypyridoxal (**3**),[7] its *N*-methochloride (**4**), and pyridoxal 5′-sulfate (**7**).[8] The phosphonate **8** was synthesized in this laboratory by C. N. Han.[9] Pyridoxal 5′-phosphate (**6**) was purchased from Sigma.

Experimental Procedure. Stock solutions of the aldehyde were prepared in water, usually at a concentration of 5×10^{-4} M. Aliquots were pipetted into volumetric flasks and appropriate amounts of the amine or amino acid component, together with buffer salts, were added. The final ionic strength was maintained at 0.2 when possible. However, solutions containing a very high concentration of the amine component (up to 1.0 M and up to 13.5 M for NH_3) were sometimes needed to permit evalu-

(1) A preliminary report appeared: *Fed. Proc., Fed. Am. Soc. Exp. Biol.* 1977, *36*, 855. A few of the data cited here also appear in ref 6.

(2) Nagano, K.; Metzler, D. E. *J. Am. Chem. Soc.* **1967**, *89*, 2891.
(3) Johnson, R. J.; Metzler, D. E. *Methods Enzymol.* **1970**, *18A*, 433.
(4) Harris, C. M.; Johnson, R. J.; Metzler, D. E. *Biochim. Biophys. Acta* **1976**, *421*, 181.
(5) Metzler, D. E.; Harris, C. M.; Johnson, R. J.; Siano, D. B.; Thomson, J. A. *Biochemistry* **1973**, *12*, 5377.
(6) Metzler, D. E.; Harris, C. M.; Reeves, R. L.; Lawton, W. H.; Maggio, M. S. *Anal. Chem.* **1977**, *49*, 864A.
(7) Iwata, C. W. *Biochem. Prep.* **1968**, *12*, 117.
(8) Yang, In-Yu; Khomutov, R. M.; Metzler, D. E. *Biochemistry* **1974**, *13*, 3877.
(9) Han, C. N. Ph.D. Dissertation, Iowa State University, 1977.

0002-7863/80/1502-6075$01.00/0